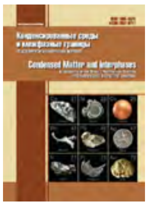

ISSN 1606-867X (Print)
ISSN 2687-0711 (Online)
Condensed Matter and Interphases
Kondensirovannye Sredy i Mezhfaznye Granitsy
https://journals.vsu.ru/kcmf/

Original articles

Research article
https://doi.org/10.17308/kcmf.2021.23/3429

Sol-gel synthesis, crystal structure and magnetic properties of nanocrystalline praseodymium orthoferrite

Bui Xuan Vuong[1], Nguyen Anh Tien[2]✉

[1]Faculty of Natural Sciences, Sai Gon University, Ho Chi Minh City 700000, Vietnam

[2]Faculty of Chemistry, Ho Chi Minh City University of Education, Ho Chi Minh City 700000, Vietnam

Abstract

In this work, nano-sized crystalline praseodymium orthoferrite was successfully synthesized via sol-gel method using water – methanol co-solvent. Single-phase $PrFeO_3$ nanoparticles were formed after annealing the precursors at 650, 750, 850, and 950 °C during 60 min. The crystal size, lattice volume and coercivity (H_c) of nanocrystalline $PrFeO_3$ increase with the annealing temperature. The obtained praseodymium orthoferrite exhibited paramagnetic properties with H_c = 28 – 34 Oe.

Keywords: Sol-gel synthesis, Methanol, Praseodymium orthoferrite, Magnetic property

For citation: Bui X. V., Nguyen A. T. Sol-gel synthesis, crystal structure and magnetic properties of nanocrystalline praseodymium orthoferrite. *Kondensirovannye sredy i mezhfaznye granitsy = Condensed Matter and Interphases.* 2021;23(2): 196–203. https://doi.org/10.17308/kcmf.2021.23/3429

Для цитирования: Буи Х. В., Нгуен А. Т. Золь-гель синтез, кристаллическая структура и магнитные свойства нанокристаллического ортоферрита празеодима. *Конденсированные среды и межфазные границы*. 2021;23(2): 196–203. https://doi.org/10.17308/kcmf.2021.23/3429

✉ Nguyen Anh Tien, e-mail: tienna@hcmue.edu.vn

1. Introduction

Amongst nano-sized metal oxide semiconductors, rare earth orthoferrites $AFeO_3$ (A = La, Y, Pr, Sm, Ho) have been studied for application in many fields such as inorganic dyes, optical catalysts, gas sensors, magnetic materials or electrodes for Li-ion battery [1–8]. The properties of this type of materials depend on not only the particle size and morphology, but also the dopant concentration and preparation methods [5–9].

Recently, the sol-gel method has been used for preparation of $AFeO_3$ orthoferrite nanomaterials owing to many advantage of this method: low annealing temperature, narrow particle size distribution, high purity, facile synthesize highly doped $AFeO_3$ materials, [1–3, 10–12]. However, the challenge of this method lies in the selection of appropriate organic polymer for gel formation and the experimental time is usually prolonged. In previous works [13–14], orthoferrite $AFeO_3$ (A = Nd and Ho) nanomaterials of particle size < 100 nm were synthesized by co-precipitation method using hot ethanol via the hydrolysis of A(III) and Fe(III) cations in hot water (T > 95 °C) and NH_3 5 % solution as the precipitant. Methanol and ethanol have similar dipole moments (($\mu(C_2H_5OH)$ = 1.66 D, $\mu(CH_3OH)$ = 1.69 D) [15], which are lower than that of water ($\mu(H_2O)$ = 1.85 D) [16]. Meanwhile, the viscosity of CH_3OH ($5.9\cdot10^{-4}$ Pa· s) is lower than that of C_2H_5OH ($1.2\cdot 10^{-3}$ Pa·s), and is also very low compared to organic polymers [15]. As a result, the interaction between A(III) and Fe(III) cations with CH_3OH is smaller than with C_2H_5OH, which leads to the decrease of the size of orthoferrite $AFeO_3$ particles synthesized by sol-gel method using methanol.

In this work, the formation, as well as structural and magnetic properties of nano-sized orthoferrite praseodymium (o-$PrFeO_3$) prepared by sol-gel method using methanol have been studied and characterized.

2. Experimental and methods

All solvents and chemicals for the synthesis of used nanocrystalline praseodymium orthoferrite were purchased and used as-received: $Pr(NO_3)_3\cdot 6H_2O$ (99.8 % purity, Merck), $Fe(NO_3)_3\cdot 9H_2O$ (99.6 % purity, Sigma-Aldrich), methanol absolute (99.7 % purity, d = 0.792 g/mL), ammonia solution (Xilong purity, 85 %, d = 0.901 g/mL).

A mixture of $Pr(NO_3)_3\cdot 6H_2O$ and $Fe(NO_3)_3\cdot 9H_2O$ (1:1 mol to mol ratio) was dissolved in 50 mL solvent of H_2O – CH_3OH (1:1, V/V). The mixture solution was then added dropwise to a round-bottom flask containing 150 mL boiling H_2O – CH_3OH co-solvent (T ~ 85 °C). The slow addition of Pr (III) and Fe (III) mixture to the co-solvent at 85 °C would increase the hydrolysis process, thus hinder and control the particle size of orthoferrite $PrFeO_3$. Details of optimized conditions can be found in previous reports on the synthesis of $LnFeO_3$ (Ln = Y, La, Nd) orthoferrites [17–19]. The system continued to be refluxed for an additional 30 minutes before cooling down to ~ 30 °C, resulted in a brownish-yellow mixture. By refluxing, the solvent volume was maintained and the diffusion of toxic CH_3OH vapor to the environment could be minimized. Next, NH_3 5 % solution was added dropwise to the system until pH ~ 9÷10 (tested by pH paper). The system was stirred for 30 minutes, then vacuum filtered. After removing all the filtrate, the residue was dry at 50 °C during 3 hours and grounded to obtain brownish-yellow powder (precursor for the synthesis of o-$PrFeO_3$).

Thermogravimetry and differential scanning calorimetry (TG-DSC) curves were recorded under dried air at the heating rate of 10 K·min^{-1}, maximum temperature 950 °C, platinum crucibles, using Labsys Evo – TG-DSC 1600 °C (France).

X-ray diffraction (XRD) patterns of $PrFeO_3$ samples were recorded using X-ray powder diffractometer (XRD, D8-ADVANCE, Germany) with CuK_α radiation (λ = 1.5406 Å), range 2θ = 10-75°, step size 0.019 °/s. Crystal size (D_{XRD}, nm) of $PrFeO_3$ samples was determined according to Debye-Scherrer equation, lattice parameters (a, b, c, V) were calculate according to previous works [12, 19-20]. Phase composition was determined by Rietveld refinement, Fullprof 2009.

The content and surface distribution of the elements (Pr, Fe, O) were studied by energy-dispersive X-ray spectroscopy (EDX and EDX-mapping), FE-SEM S-4800 (Japan). The quantitative elemental composition were taken as the average of 5 different positions of each sample.

Crystal size and morphology of $PrFeO_3$ samples were characterized by transmission electron spectroscopy (TEM), Joel JEM-1400 (Japan). The crystal size distribution of were determined by IMAGE J.

Hysteresis loop and magnetic properties including coercive force (H_c, Oe), remanent magnetization (M_r, emu/g) and saturation magnetization (M_s, emu/g) were recorded on vibrating sample magnetometer (VSM, MICROSENE EV11) under the magnetic field in the range of -21 000 Oe to +21 000 Oe.

3. Results and discussion

Fig. 1 shows the TG-DSC curves of precursors for the synthesis of o-$PrFeO_3$ nanomaterial. The total mass loss from room temperature to 950 °C was 23.67 %. This result proves the formation of bonds between Pr(III) and Fe(III) cation with CH_3- group in the precipitate [21]. Indeed, if this precipitate had only included $Pr(OH)_3$↓ and $Fe(OH)_3$↓, mass loss deduced from equation (1) would have been 18.07 %.

$$Fe(OH)_3 + Pr(OH)_3 \rightarrow PrFeO_3 + 3H_2O \quad (1)$$

The mass loss by decomposition of M^{3+}–CH_3 (M = Pr, Fe) bonds corresponds to the exothermic peak at 270.56 °C on the DSC curve (Fig. 1). The endothermic peaks at 113.37 and 358.52 °C are the dehydrate and decomposition of praseodymium (III) and iron (III) hydroxides. Similar results were also observed in previous works [13, 19] for $HoFeO_3$ and $NdFeO_3$ orthoferrite. The exothermic peak at 617.31 °C correspond to the phase formation of $PrFeO_3$ orthoferrite from Pr_2O_3 and Fe_2O_3 according to equation (2). This inference is in good agreement with the mass change on the TG curve (there were no observable changes in the sample's mass from ~650 °C). From the TG-DSC results, the sample was annealed at 650, 750, 850, and 950 °C for 60 min to characterize the structural properties of $PrFeO_3$ crystals by XRD.

$$Fe_2O_3 + Pr_2O_3 \rightarrow 2PrFeO_3 \quad (2)$$

XRD patterns of praseodymium orthoferrite precursor after annealing at different temperatures for 60 min were shown in Fig. 2. The results give single phase orthorhombic $PrFeO_3$. All obtained peaks match well with the standard peaks of $PrFeO_3$ (JCPDS: 74-1472), without any observable oxide peaks such as Pr_2O_3, Pr_6O_{11} or Fe_2O_3. The degree of crystallinity and crystal phase content of $PrFeO_3$ samples increased with the annealing temperature, however, this increment was not linear (Table 1). The crystallinity of the sample annealed at 750 °C (592.04 cts) and that annealed at 950 °C (614.66 cts) were approximate, but the $PrFeO_3$ crystal phase content of the sample

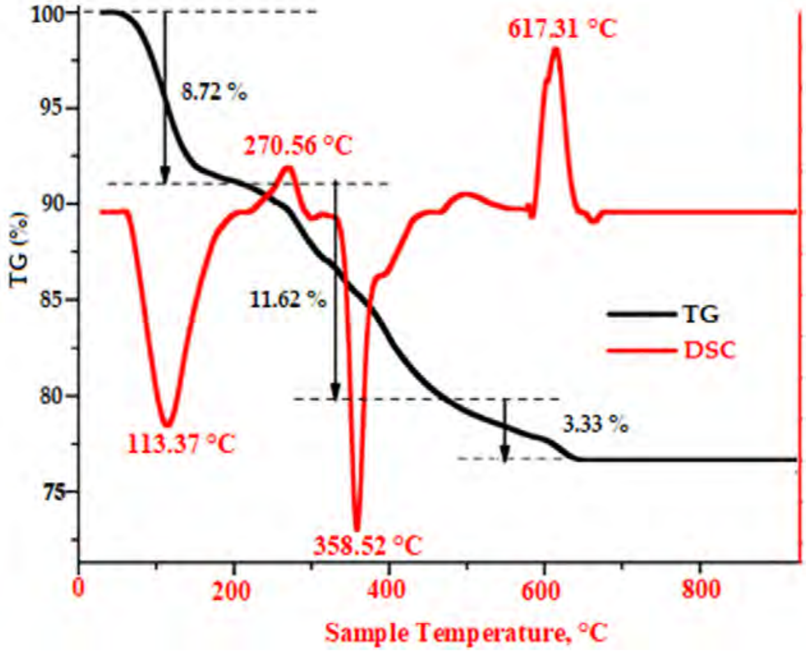

Fig. 1. TG-DSC curves of the dried gel powders

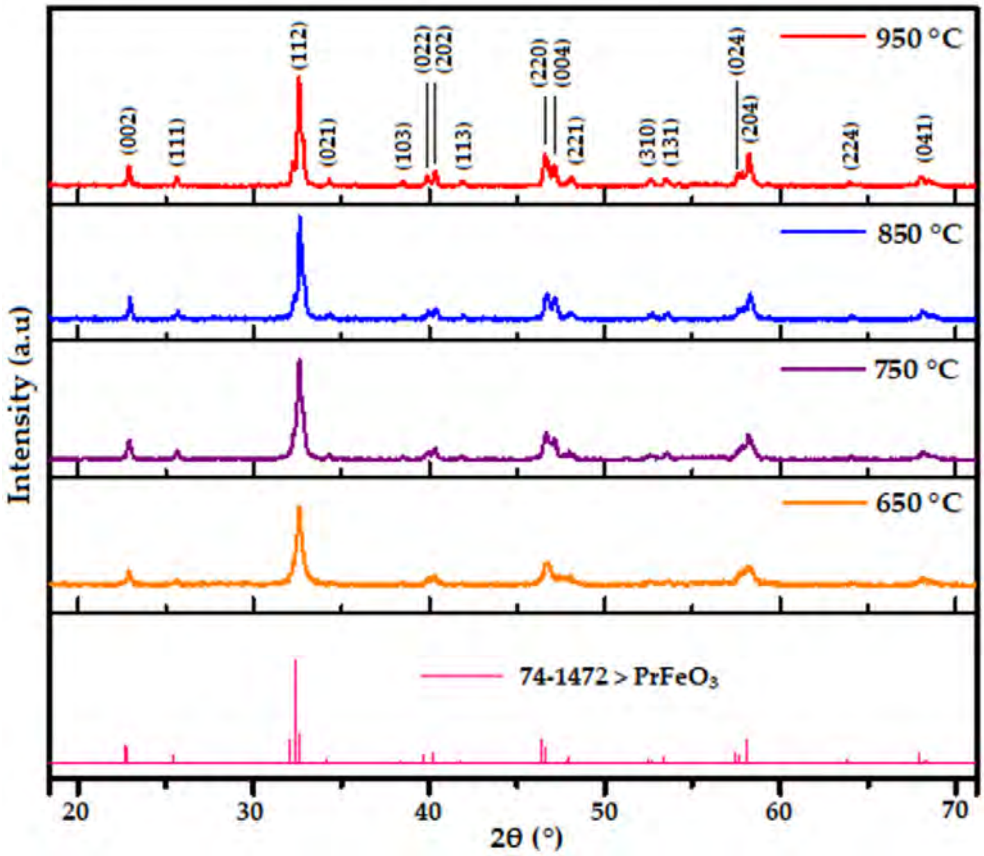

Fig. 2. PXRD patterns of $PrFeO_3$ nanopowders annealed at 650, 750, 850, and 950 °C for 60 min

Table 1. Characteristics of $PrFeO_3$ samples annealed at different temperatures for 60 min

T	650 °C	750 °C	850 °C	950 °C
2θ, °	32.6092	32.5659	32.6185	32.5584
Height, cts	288.26	592.04	490.86	614.66
Crystal phase, %	68.8	93.4	80.5	89.7
Amorphous phase, %	31.2	6.6	19.5	10.3
FWHM, °	0.1309	0.1683	0.1122	0.1122
d-spacing, Å	2.74604	2.74960	2.74529	2.75022
D, nm	62.5	48.6	73.0	73.0
a, Å	5.4556	5.4521	5.4509	5.4501
b, Å	5.5753	5.5840	5.6206	5.6218
c, Å	7.8113	7.7245	7.8169	7.8145
V, $Å^3$	237.59	235.17	239.49	239.43
H_c, Oe	28.0	30.8	33.7	–
M_r, emu/g	0.22	0.13	0.76	–
M_s, emu/g	0.24	1.10	0.73	–

annealed at 750 °C was much higher than the others. The full-width at half maximum (FWHM, °) of the sample annealed at 750 °C was the widest, leading to the smallest Debye-Scherrer crystal size (D_{XRD} = 48.6 nm) and lattice volume (V = 235.17 $Å^3$) (Table 1). Thus, it can be assumed that 750 °C for 60 min is the appropriate conditions for the formation of single phase praseodymium orthoferrite (o-$PrFeO_3$) by sol-gel method using water-methanol co-solvent.

From the EDX and EDX-mapping analysis of $PrFeO_3$ sample annealed at 750 °C, only praseodymium, iron and oxygen peaks were observable without any other signals of impurity elements (Fig. 3). The averages of weight percentage and atomic percentage of the elements Pr, Fe, O from five different positions are shown in Table 2. The obtained results are consistent with expected chemical composition (Table 2).

Particle size and morphology of $PrFeO_3$ powder annealed at 750 °C are shown in the TEM image (Fig. 4a**).** The obtained particles have slightly angular spherical shape with the size mostly in the range of 20–60 nm (Fig. 4b). Average size calculated by IMAGE J was 46.28 nm. This result is rather close to the crystal size by Debye-Scherrer equation (D_{XRD} = 48.6 nm) (Table 1).

Field dependence of the magnetization of $PrFeO_3$ nanomaterials at 300K are shown in Fig. 5. The coercive force (H_c = 20.8 ÷ 30.7 Oe) and saturation magnetization (M_r = 0.13 ÷ 0.76 emu/g) (Table 1) of all three $PrFeO_3$ samples in this work are much lower than those of $PrFeO_3$ prepared by co-precipitation method reported by Sudandararaj T. S. A. et. al. [22] (H_c = 505.45 Oe, M_r = 27.63 emu/g). The low value of H_c and

Table 2. EDX analysis of $PrFeO_3$ nano-sized powders annealed at 750 °C

Pr		Fe		O	
Wt%	At%	Wt%	At%	Wt%	At%
56.39	21.02	22.35	18.28	21.36	60.70

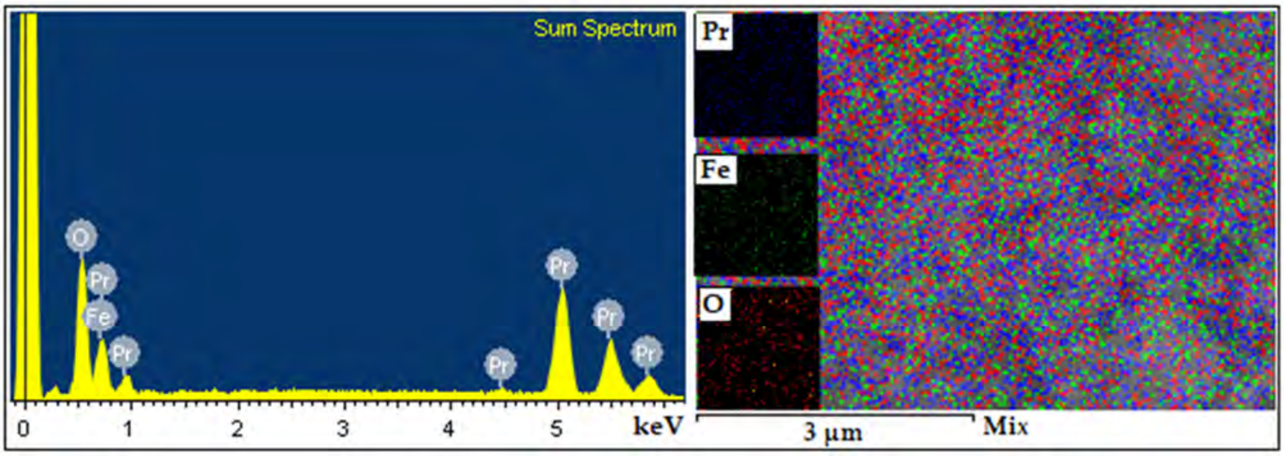

Fig 3. EDX and EDX-mapping images of $PrFeO_3$ sample annealed at 750 °C

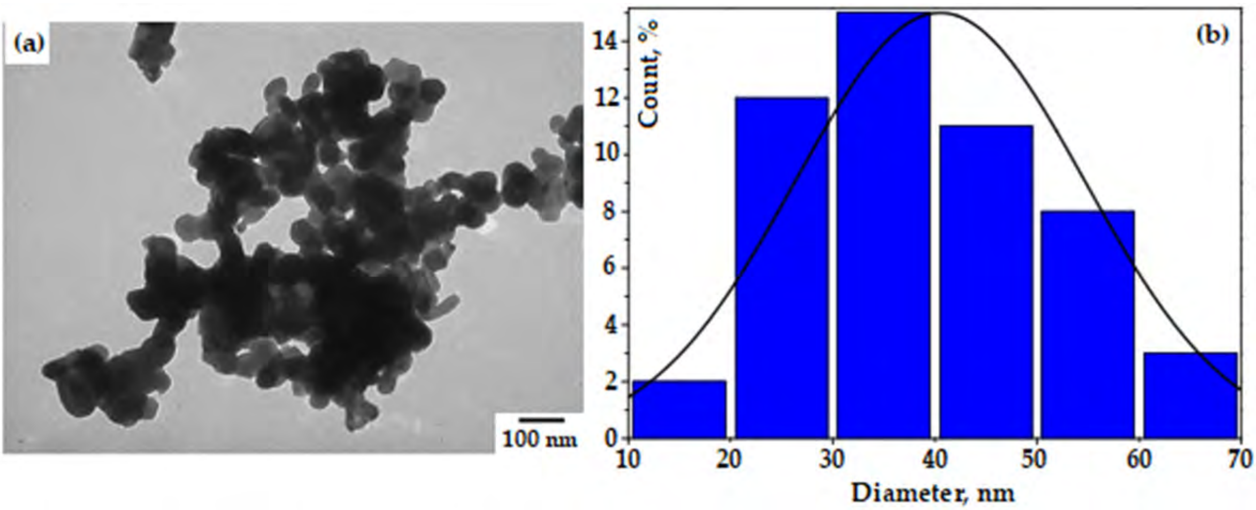

Fig. 4. (a) TEM image of $PrFeO_3$ sample annealed at 750 °C and (b) Particle size distribution

M_r could be originated from the homogeneity in shape and size of the $PrFeO_3$ nanoparticles with clear particle boundaries (see Fig. 4) while in the TEM image of the corresponding $PrFeO_3$ in [22], the particle boundaries are not observable with severe aggregation that joined the entire area of the material despite the particle size of 36.0 nm (by Image J).

Most interestingly, the magnetic parameters of $PrFeO_3$ nanomaterials changed irregularly with the annealing temperature (Table 1). The $PrFeO_3$ sample annealed at 750 °C has the lowest M_r (0.13 emu/g) while its M_s (1.10 emu/g) has the highest value. This can be ascribed by the highest crystallinity and crystal phase content of the $PrFeO_3$ sample annealed at 750 °C (see Table 1) which decreased the magnetocrystalline anisotropy of the material, leading to the rise in M_s and the decreased in M_r [23–24].

Thus, with low H_c, M_r and high M_s, obtained $PrFeO_3$ nanomaterials are soft magnetics that can be applied as material working under the external field as transformer cores, electromagnet cores, and conductive cores [24].

4. Conclusions

In this study, nanocrystalline praseodymium orthoferrite (o-$PrFeO_3$) was successfully synthesized by sol-gel method using water-methanol co-solvent. The $PrFeO_3$ nanocrystal formed after annealing the precursor at different temperatures (650, 750, 850, and 950 °C) for 1 hour. The crystal size of $PrFeO_3$ samples are in the range of 45÷70 nm (XRD, TEM). The $PrFeO_3$ sample annealed at 750 °C had the highest crystallinity (592.04 cts) and crystal phase content (93.4 %) (XRD) with smallest particle size (46.28 nm, TEM). The obtained $PrFeO_3$ nanomaterials are soft magnetic materials with low coercive force and remanent magnetization, high saturation magnetization.

Contribution of the authors

The authors contributed equally to this article.

Conflict of interests

The authors maintain that they have no conflict of interest to be described in this communication.

References

1. Opuchovic O., Kreiza G., Senvaitiene J., Kazlauskas K., Beganskiene A., Kareiva A. Sol-gel synthesis, characterization and application of selected sub-microsized lanthanide (Ce, Pr, Nd, Tb) ferrites. *Dyes and Pigments*. 2015;118: 176–182. https://doi.org/10.1016/j.dyepig.2015.03.017

2. Luxova J., Sulcova P., Trojan M. Influence of firing temperature on the color properties orthoferrite $PrFeO_3$. *Thermochimica Acta*. 2014;579: 80–85, http://dx.doi.org/10.1016/j.tca.2014.01.017

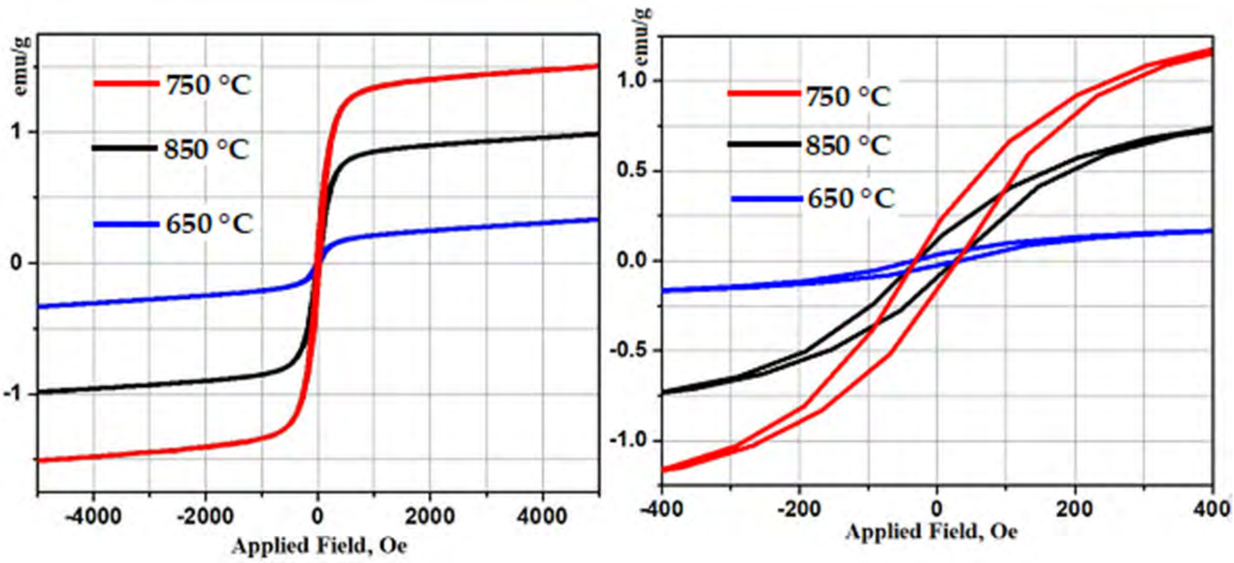

Fig. 5. Field dependence of the magnetization of $PrFeO_3$ nanoparticles annealed at 650, 750, and 850 °C for 1 h

3. Kondrashkova I. S., Martinson K. D., Zakharova N. V., Popkov V. I. Synthesis of nanocrystalline $HoFeO_3$ photocatalyst via heat treatment of products of glycine-nitrate combustion, *Russian Journal of General Chemistry*. 2018;88(12): 2465–2471. https://doi.org/10.1134/S1070363218120022

4. Fergus J. W. Perovskite oxides for semiconductor-based gas sensors. *Sensors and Actuators B: Chemical*. 2007;123(2): 1169–1179. https://doi.org/10.1016/j.snb.2006.10.051

5. Oemar U., Ang P., Hidajat K., Kawi S. Promotional effect of Fe on perovskite $LaNi_xFe_{1-x}O_3$ catalyst for hydrogen production via steam reforming of toluene. *International Journal Hydrogen Energy*. 2013;38(14): 5525–5534. https://doi.org/10.1016/j.ijhydene.2013.02.083

6. Mir F. A., Sharma S., Kumar R. Magnetizations and magneto-transport properties of Ni-doped PrFeO3 thin films. *Chinese Physics B*. 2014;23(4): 048101. https:/doi.org/10.1088/1674-1056/23/4/048101

7. Zhang L., Zhang X., Tian G., Zhang Q., Knapp M., Ehrenberg H., Chen G., Shen Z., Yang G., Gu L. Lithium lanthanum titanate perovskite as an anode for lithium ion batteries. *Nature communications*. 2020;11(1): 1–8. https://doi.org/10.1038/s41467-020-17233-1

8. Liu J., Sheha E., El-Dek S. I., Goonetilleke D., Harguindeguy M., Sharma N. $SmFeO_3$ and Bi-doped $SmFeO_3$ perovskites as an alternative class of electrodes in lithium-ion batteries. *CrystEngComm*. 2018;20(40): 6165–6172. https://doi.org/10.1039/c8ce00780b

9. Chen Ch., Jang P. W., Kim J. S. Ferroelectric and magnetic properties of $PrFeO_3$-$PbTiO_3$ and $PrFeO_3$-$BiFeO_3$–$PbTiO_3$ thin films. *Japanese Journal of Applied Physics*. 2002;41(11B): 6777. https:/doi.org/10.1143/JJAP.41.6777

10. Pekinchak O., Vasylechko L., Lutsyuk I., Vakhula Ya., Prots Yu., Carrillo-Cabrela W. Sol-gel-prepared nanoparticles of mixed praseodymium cobaltites-ferrites. *Nanoscale Research Letters*. 2016;11: 75. https://doi.org/10.1186/s11671-016-1295-y

11. Peisong T., Xinyu X., Haifeng Ch., Chunyan L., Yangbin D. Synthesis of nanoparticulate $PrFeO_3$ by sol-gel method and its visible-light photocatalytic activity. *Ferroelectrics*. 2019;546: 181–187. https://doi.org/10.1080/00150193.2019.1592470

12. Tijare S. N., Bakardjieva S., Subrt J., Joshi M. V., Rayalu S. S., Hishita S., Labhsetwar N. Synthesis and visible light photocatalytic activity of nanocrystalline $PrFeO_3$ perovskite for hydrogen generation in ethanol-water system. *Journal of Chemical Sciences*. 2014; 126(2): 517–525. https://doi.org/10.1007/s12039-014-0596-x

13. Nguyen T. A., Nguyen L. T. Tr., Bui V. X., Nguyen D. H. T., Lieu H. D., Le L. M. T., Pham V. Optical and magnetic properties of $HoFeO_3$ nanocrystals prepared by a simple co-precipitation method using ethanol. *Journal of Alloys and Compounds*. 2020;834: 155098. https://doi.org/10.1016/j.jallcom.2020.155098

14. Nguyen A. T., Nguyen V. Y., Mittova I. Ya., Mittova V. O., Viryutina E. L., Hoang C. Ch. T., Nguyen Tr. L. T., Bui X. V., Do T. H. Synthesis and magnetic properties of $PrFeO_3$ by the co-precipitation method using ethanol. *Nanosystems: Physics, Chemistry, Mathematics*. 2020;11(4): 468–473. https://doi.org/10.17586/2220-8054-2020-11-4-468-473

15. Housecroft C. E., Sharpe A. G. *Inorganic Chemistry*, *2nd edition*. Pearson: Prentice Hall; 2005.

16. Klein D. *Organic Chemistry, 2nd edition*. Wiley; 2016. chapter 13.

17. Nguyen A. T., Mittova I. Ya., Almjasheva O. V., Kirillova S. A., Gusarov V. V. Influence of the preparation condition on the size and morphology of nanocrystalline lanthanum orthoferrite. *Glass Physics and Chemistry*. 2008;34(6): 756–761. https://doi.org/10.1134/S1087659608060138

18. Nguyen A. T., Mittova I. Ya., Almjasheva O. V. Influence of the synthesis condition on the particle size and morpholopgy of ytrrium orthoferrite obtained. *Russian Journal of Applied Chemistry*. 2009;82(11): 1915–1918, https://doi.org/10.1134/S1070427209110020

19. Nguyen T. A., Pham V., Pham Th. L., Nguyen L. T. Tr., Mittova I. Ya., Mittova V. O., Vo L. N., Nguyen B. T. T., Bui V. X., Viryutina E. L. Simple synthesis of $NdFeO_3$ by the so-precipitation method based on a study of thermal behaviors of Fe (III) and Nd (III) hydroxides. *Crystals*. 2020;10: 219. https://doi.org/10.3390/cryst10030219

20. Abdellahi M., Abhari A. Sh., Bahmanpour M. Preparation and characterization of orthoferrite $PrFeO_3$ nanoceramic. *Ceramics International*. 2016;42(4): 4637–4641. http://dx.doi.org/10.1016/j.ceramint.2015.12.027

21. Brinker C. J., Scherer G. W. (eds.) *Sol-gel science: the physics and chemistry of sol-gel processing*. I Boston: Academic Press; 1990. 908 p.

22. Sudandararaj T. A. S., Kumar G. S., Dhivya M., Eithiraj R. D., Banu I. B. S. Spin reorientation transition in nanoscale multiferroic $PrFeO_3$ and its band structure calculation. *Journal of Alloys and Compounds*. 2020;817: 152747. https://doi.org/10.1016/j.jallcom.2019.152747

23. Nada F. A., Ahmed G., Ekram H. E-A. *Perovskite nanomaterials: Synthesis, characterization, and appli-*

cations, 1st ed. / Likun Pan, Guang Zhu (eds.). London: InTechOpen; 2016. Chapter 4, pp. 107–151. https://doi.org/10.5772/61280

24. Cullity B. D., Graham C. D. *Introduction to magnetic materials, 2nd ed*. Canada: John Wiley & Sons, Inc., Publication; 2009. https://doi.org/10.1002/9780470386323

Information about the authors

Xuan Vuong Bui, PhD in Chemistry, Lecturer of Faculty of Natural Sciences, Sai Gon University, Ho Chi Minh City, Vietnam; e-mail: bxvuong@sgu.edu.vn. ORCID iD: https://orcid.org/0000-0002-3757-1099.

Anh Tien Nguyen, PhD in Chemistry, Chief of General and Inorganic Chemistry Department, Ho Chi Minh City University of Education, Vietnam; E-mail: tienna@hcmue.edu.vn. ORCID iD: http://orcid.org/0000-0002-4396-0349.

Received 13 April 2021; Approved after reviewing 30 April 2021; Accepted 15 May 2021; Published online 25 June 2021.